Hindawi
Shock and Vibration
Volume 2018, Article ID 3619257, 8 pages
https://doi.org/10.1155/2018/3619257

Research Article

Experimental Study of a Broadband Parametric Acoustic Array for Sub-Bottom Profiling in Shallow Water

Ke Qu,[1,2] **Binbin Zou**,[3] **Jingjing Chen**,[3] **Yingge Guo**,[3] **and Runtian Wang**[3]

[1]*Guangdong Province Key Laboratory for Coastal Ocean Variation and Disaster Prediction, Guangdong Ocean University, Zhanjiang 524088, China*
[2]*College of Electronics and Information Engineering, Guangdong Ocean University, Zhanjiang 524088, China*
[3]*Shanghai Acoustic Laboratory, Chinese Academy of Science, Shanghai 200032, China*

Correspondence should be addressed to Binbin Zou; zoubb@mail.ioa.ac.cn

Received 24 June 2018; Revised 10 November 2018; Accepted 22 November 2018; Published 25 December 2018

Academic Editor: Zhixiong Li

Broadband parametric acoustic arrays appear to offer advantages for shallow water sub-bottom profiling. In this paper, the performance of a broadband parametric acoustic array system was experimentally evaluated. In tank experiments using the nonlinear parabolic wave (KZK) equation, the directivity, source level, parametric acoustic array length, and penetration depth were evaluated. Based on Berktay's far-field solution, the system's emission signal was designed. According to sea trials of the broadband parametric acoustic array system as designed, a clear sub-bottom profile was obtained. Moreover, buried pipelines in the seabed were effectively detected, verifying the system's effectiveness.

1. Introduction

In traditional sub-bottom profiling systems, due to the limitations of the linear sound source, the detector beam is relatively wide and has low resolution. To obtain a low-frequency sound source with high directivity, a transducer with a larger aperture is needed. Therefore, it is difficult to satisfy the device portability requirement in actual application. Based on a parametric acoustic array system of nonlinear sound sources, a small-aperture broadband beam with low frequency, high directivity, and without sidelobes can be realized. The parametric acoustic array system is very suitable for high-resolution detection of seabed stratigraphic profiles and represents an important development direction in sub-bottom profile detection technology [1].

The basic theory of parametric acoustic arrays was first proposed by Westervelt in the 1960s [2, 3]. Later, Berktay further deduced the relative emission theory of parametric acoustic arrays and promoted their application [4]. Because it offers a low-frequency sound source with a narrow beam and no sidelobes, the technology has been used in sub-bottom profiling [5], industrial flaw detection [6], medical examination [7], biological detection [8], target tracking [9], and underwater acoustic communication [10, 11]. However, its most mature application in underwater acoustics is still the sub-bottom profiler [12–14]. To satisfy measurement requirements at different depths, a single-frequency difference frequency signal is generally used in current parametric array sonar systems, and the original frequency is relatively low. During offshore detection, because the frequency is low, the parametric array will be truncated, which impacts far-field directivity. Moreover, because the signal bandwidth is insufficient, it is difficult to carry out high-resolution detection on the seabed.

To meet the demand for high-resolution offshore detection, especially for detecting profiles within 10 m of the seafloor sediment and detecting buried objects, a broadband parametric array system was designed in this study. By using a 20–30 kHz difference frequency signal generated by the 300 kHz original frequency, the vertical resolution can be effectively improved. Based on Berktay's envelope modulation theory and the KZK (Khokhlov-Zabolotskaya-Kuznetsov) equation combined with tank experiments, the performance of the broadband difference frequency sound source was evaluated under various conditions, and the detection effect was deduced. Finally, sea trials were carried

out for the system, and effective detection results were obtained. While parametric acoustic array has been received considerable attention over the past decade, relatively few engineering details have surfaced about a whole broadband parametric acoustic array system [15–20]. The key engineering issues and performance of the whole broadband parametric acoustic array system are presented in this paper.

2. Theory

In the linear theory, there is no interaction when two sound waves at different frequencies are superposed. The total sound field is equal to the linear superposition of the two sound pressures. In the nonlinear theory, for sound waves f_1 and f_2 at different frequencies in a nondispersive medium, each sound wave is disturbed by the other one when it propagates in the medium. Interaction occurs when two sound waves at different frequencies are superposed. Besides the original frequency wave, the sum frequency wave at frequency $f_1 + f_2$, the difference frequency wave at frequency $f_1 - f_2$, and harmonic frequency waves at frequencies nf_1 and nf_2 ($n = 2, 3, \ldots$) all exist. During propagation, the original frequency wave generates acoustic scattering continuously. This forward scattering is repeatedly superposed on the sound scattering produced earlier, and as a result, it is gradually enhanced. The process can be regarded as involving a volume array consisting of virtual sources of various secondary sound fields in space. This volume array is called a parametric array. In the secondary sound field of the parametric array, the difference frequency sound field has attracted the most attention in sonar engineering.

Let us assume that the medium is an ideal fluid and that only one attenuation coefficient is introduced to characterize the attenuation effect of the medium on the sound wave. It is also assumed that the original frequency wave and the difference frequency wave propagate with small amplitude. The continuity equation, momentum conservation equation, and equation of state can be combined, and a second-order approximation, the Westervelt nonlinear equation, can be deduced [3]:

$$\nabla^2 p - \frac{1}{c_0^2}\frac{\partial^2 p}{\partial^2 t} = -\rho_0 \frac{dq}{dt}, \tag{1}$$

where p is the sound pressure, c_0 is the sound speed in the medium, ρ is the medium density, t is the time, and q is the source strength density. Based on the study of the input broadband signal, Berktay proposed an amplitude modulation method. It is assumed that the emission signal is $p(t) = p_0 E(t)\cos(\omega_0 t)$, where p_0 is the amplitude of the sound source at the original frequency and $E(t)$ is the envelope of the emission signal, whose frequency should be much less than the original frequency ω_0. Then, the sound pressure at position x on the sound axis can be expressed as follows:

$$p(t) = P_0 e^{-a_0 x} E\left(t - \frac{x}{c_0}\right)\cos(\omega_0 t - k_0 x). \tag{2}$$

By substituting into equation (1), the sound pressure of the difference frequency at position r on the far-field sound axis can be obtained:

$$p_d(r,t) = \frac{p_0^2 s\beta}{16\pi\rho c_0^4 \alpha_0 r}\frac{\partial^2}{\partial t^2}E^2\left(t - \frac{r}{C_0}\right), \tag{3}$$

where β is the nonlinear coefficient, s is the area of the transmitting transducer, and α_0 is the attenuation coefficient of the original frequency wave. Berktay's theory can be used only to calculate the far-field solution on the sound axis. The KZK equation can more completely describe the nonlinear effect of the sound field at different positions, including near and nonaxial sound fields:

$$\frac{\partial^2 p}{\partial z \partial \tau} = \frac{C_0}{2}\Delta p + \frac{\delta}{2c_0^3}\frac{\partial^3 p}{\partial \tau^3} + \frac{\beta}{2\rho_0 c_0^3}\cdot\frac{\partial^2 p^2}{\partial \tau^3}, \tag{4}$$

where $\tau = t - z/c_0$ is the delay time and Δ is a Laplace operator. In the following discussion, the emission signal of the parametric array is designed according to equation (3), and the simulation result is analyzed by equation (4).

Equation (3) shows that the sound pressure amplitude of the difference frequency wave on the axis is proportional to the second-order derivative of the square of the envelope signal versus time and that the results are valid in the weak nonlinear far field. Assuming constant total power and amplitude modulation, compared with a dual-frequency parametric array, the gain of the difference frequency signal of the broadband parametric array has improved by 2.1–6.0 dB [21]. Equation (3) also illustrates that the spectral range of the difference frequency signal can theoretically double the emission signal envelope. As a relatively high-frequency signal, the emission signal can easily generate a wider broadband using current underwater acoustic transducer technology. As a relatively low-frequency signal, the difference frequency signal also has wide broadband and sharp directivity, which cannot be achieved by the common low-frequency transducer.

3. Tank Experiments

To study the performance of the broadband parametric array system, several experiments were carried out in a water tank. Figure 1 shows that the length, width, and height of the water tank were 10 m, 5 m, and 5 m, respectively. Sound-absorbing materials were laid on the walls and bottom. The center frequency of the parametric array emission system was 310 kHz, and the bandwidth at −3 dB was 120 kHz. The transducer diameter was 10 cm, and the receiving equipment was a B&K8103. The emission depth and the receiving depth were both 1.5 m. The oscilloscope was a Tektronix 2014B. The active power filter was a NF3828, and the low-pass filter was an eighth-order Butterworth filter.

3.1. Directivity. With a small aperture, a signal with high directivity and without sidelobes was obtained. Compared with the linear system, this is the greatest advantage offered by the parametric array system. To evaluate the system's directivity, the directivity of the original frequency wave at 300 kHz was first measured. Then, according to equation (3), under excitement of the envelope at sine single frequencies of 20 kHz, 10 kHz, and 5 kHz in turn, difference frequency

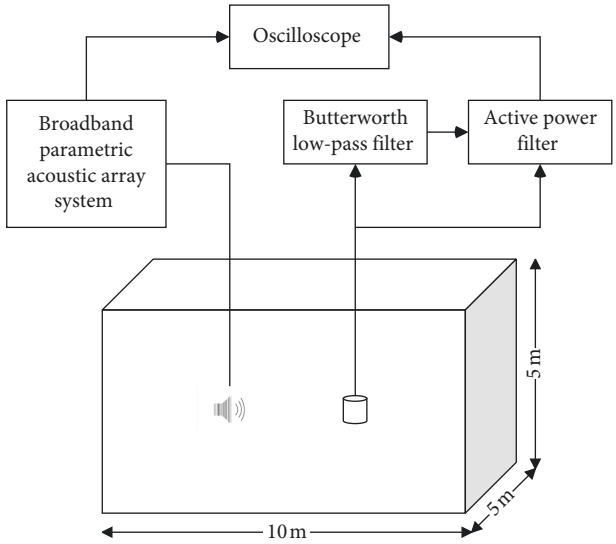

Figure 1: Sketch of measurement system.

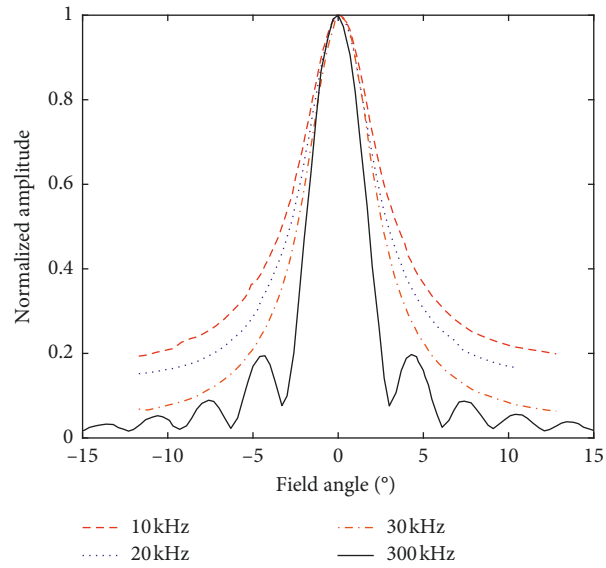

Figure 2: Directivity of the original frequency and difference frequency signals.

signals at 40 kHz, 20 kHz, and 5 kHz were obtained, and the directivity was also measured. Figure 2 shows the normalized amplitudes of the original frequency wave and the difference frequency wave. The difference frequency wave maintained the narrow-beam performance of the original frequency wave at 300 kHz, or in other words, the field angle at −3 dB of the original frequency wave was about 2.6° at 40 kHz. At a frequency of 20 kHz, it was about 3.4°, and at 10 kHz, approximately 4°. The difference frequency wave is generated by interaction with the original frequency wave in the medium. When the frequency of the original frequency wave is high, that is, the field angle of the transmitting transducer is narrow and the beam angle is small, the interaction region will be narrow. Moreover, the virtual source array is generally long in the diffusion model. The difference frequency wave can maintain the sharp directivity of the original frequency wave.

The beam angle of the parametric array can be estimated by the following formula:

$$\theta_{-3\mathrm{dB}} \approx 4\sqrt{\frac{\alpha_1 + \alpha_2 - \alpha}{2k_d}}, \tag{5}$$

where α_1 and α_2 are the sound attenuation coefficients of the original frequency, α is the sound attenuation coefficient of the difference frequency, and k_d is the wavenumber of the difference frequency. Equation (5) shows that the higher the frequency of the difference frequency wave, the narrower the beam angle becomes, which accords well with experimental results. Because of the high directivity of the sound wave, the footprint of the wave beam on the seabed is smaller, and the horizontal resolution of the device is improved. Moreover, it is beneficial for suppressing reverberation.

3.2. Source Level. A defect of parametric array technology is its low conversion efficiency. Due to the lower source level of the difference frequency, this needs to be taken into special consideration in practical applications. Assuming an average instantaneous electric power of 3200 W and an original frequency source level of 232 dB, the sound pressures of the difference frequency signal at 10 kHz, 20 kHz, 30 kHz, and 40 kHz in the axial direction 5.6 m away from the transmitting transducer were measured. Figure 3 shows the source levels of the difference frequency signal. The test results in tank experiments were basically consistent with the simulation results using the KZK equation. In practical application, the conversion efficiency is slightly lower at lower difference frequencies. It is worth mentioning that due to tank size limitations, the parameter array length was not fully expanded when the measured distance was 5.6 m. Figure 3 shows the simulation results using the KZK equation when the parametric array is completely expanded in an infinite space. The conversion efficiency is higher than when the parametric array length is not fully expanded.

3.3. Parametric Array Length. The sound field of the parametric array is an accumulation field. To form completely, it requires a certain distance, which is called the array length. The parametric array length is an important design parameter for parametric arrays. Generally, only when the measured target is outside the specified distance is the sonar of the parametric array in its optimal working condition. When the parametric array is not fully expanded, the source level and directivity will both be influenced. According to equation (3), the original frequency wave at 300 kHz was superposed on the single-frequency sine envelope signal at 15 kHz to obtain the difference frequency signal at 30 kHz. At an average instantaneous electric power of 3200 W, Figure 4 shows the simulated and measured results for the source level of the difference frequency signal at different positions. The simulation results are basically the same as the measured results, with a stable value of the difference frequency source level in the far field of 194 dB. According to the evaluation method for parametric array length proposed

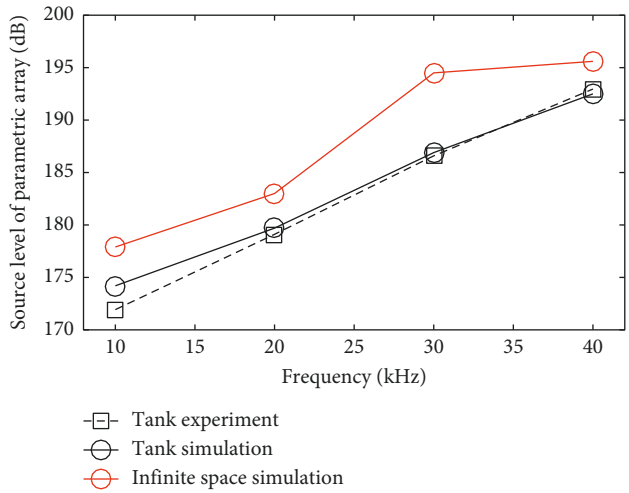

Figure 3: Source levels of the parametric array. The density of water is 1 kg/m^3, and the sound absorption coefficients at 300 kHz, 40 kHz, 30 kHz, 20 kHz, and 10 kHz are 23.4 dB/km, 0.416 dB/km, 0.234 dB/km, 0.104 dB/km, and 0.026 dB/km, respectively, at 15°C.

by Moffett and Mellen [22], when the difference between the source levels in the near and far fields is less than 1 dB, it is considered that the parametric array at the position has completely formed. During the measurement, a source level that fluctuates within about 0.5 dB is considered to be stable, and the parametric array is considered to be completely formed. At 194 dB, the corresponding array length was 19.25 m. This design broadband parametric array length is well suited to offshore detection and can effectively avoid truncation of the parametric array.

3.4. Penetration Depth. By the sonar equation, the operating distance can be estimated:

$$\mathrm{SL} - 2\mathrm{TL} + \mathrm{TS} = \mathrm{NL} - \mathrm{DI} + \mathrm{DT}, \tag{6}$$

where SL is the source level, TL is the transmission loss, TS is the target strength, NL is the noise level, DI is the directivity index, and DT is the detection threshold. When the source level of the original frequency is 232 dB, it is assumed that the sea state is at level 2-3, the noise spectrum level is 37 dB at 300 kHz, and the bandwidth is 120 kHz. DT and DI are 6 dB and 16 dB, respectively. At 15°C, the corresponding sound attenuation coefficient is 23.4 dB/km. Because the working range of the acoustic wave at the original frequency is consistently greater than 1 km, when the broadband parametric array sonar is applied, the sound wave at the original frequency can be used to perform depth sounding on the shallow seabed. Because the original frequency beam is narrow and the frequency is high, the system is suitable for seafloor imaging within the working range.

According to the source levels shown in Figure 3, it was assumed that the water depth was 50 m, and then the penetration depth could be calculated, as shown in Table 1. The sub-bottom profile and buried objects can be detected by choosing a suitable difference frequency as needed.

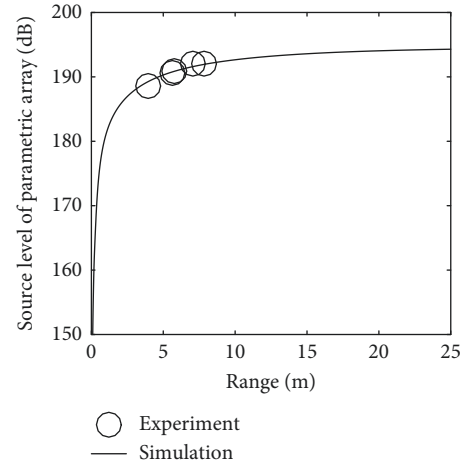

Figure 4: Parametric array length measured by the source level.

Table 1: Penetration depth of the difference frequency signal.

Frequency of difference frequency sound wave(Hz)	Average absorption coefficient in stratum (dB/λ)	Penetration depth (m)
10	0.1	14
	0.8	2
20	0.1	10
	0.8	1.4
30	0.1	11
	0.8	1.4

3.5. Broadband Difference Frequency Signal. In accordance with Berktay's far-field solution, the envelope of the emission signal was set equal to the linear modulation frequency (LMF) signal:

$$E(t) = A \cdot \mathrm{rect}\left(\frac{t}{T}\right) \cos\left[2\pi\left(f_1 t + \frac{kt^2}{2}\right)\right], \tag{7}$$

where T is the pulse width, k is the wavenumber, and $\mathrm{rect}(t/T)$ is the rectangular function:

$$\mathrm{rect}\left(\frac{t}{T}\right) = \begin{cases} 1, & 0 < t < T, \\ 0, & t \geq T. \end{cases} \tag{8}$$

The instantaneous frequency of the signal is

$$f(t) = \frac{1}{2\pi}\frac{d}{dt}\left[2\pi\left(f_1 t + \frac{kt^2}{2}\right)\right] = f_1 + kt. \tag{9}$$

When the modulation frequency range is 2.5–15 kHz, T and k are set to 0.719 ms and 1.7×10^7, respectively. Figure 5 shows the normalized frequency spectrum.

The frequency of the original frequency signal is 320 kHz, and the envelope is the LMF signal described above. Figure 6 shows the simulated and tank experimental results for the difference frequency signal acquired at the receiving end. Clearly, the experimental and simulated results are very close. The source of the small error is a certain error that occurs in the measured sound pressure on the sound axis due to the narrow beam of the parametric array.

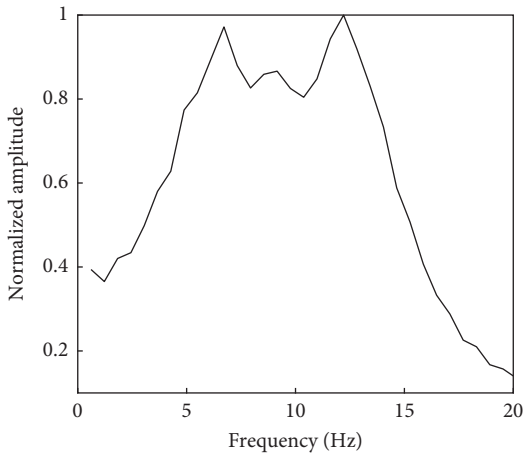

Figure 5: Normalized frequency spectrum of the emission signal envelope.

According to the frequency calculation formula (equation (3)), the frequency spectrum of the difference frequency signal will expand from the frequency spectrum of the envelope signal in the 2.5–15 kHz range to 5–30 kHz. Moreover, the amplitude at low frequency will be less than at high frequency. These characteristics are reflected in the signal from the tank experiments.

In practical application, the difference frequency signal of the echo can be used to detect sub-bottom profiles and buried objects. By introducing a suitable broadband signal-processing method, the vertical detection resolution can be effectively improved. In particular, this method is appropriate for complex layers in sediment. A previous simulation demonstrated that by using frequency spectrum modification and pulse compression technology at the receiving end, the effective resolution range of a broadband parametric array for buried objects in shallow water was 0.1 m [5].

3.6. Single-Channel Blind Signal Separation Algorithm. Generally, the transmitter-receiver of a parametric array system is a single channel. In this study, using a single-channel blind signal separation algorithm, the geoacoustic signal was extracted from ship noise and ambient ocean noise.

Let us consider the received signals as the signal S_j generated by n sources and forming an output x in the single receiver. The noise also serves as one of the signal sources, and the observable output of the receiver can be expressed as

$$x(t) = \sum_{j=1}^{n} a_j S_j(t), \tag{10}$$

where a_j is the mixing coefficient. By the single-channel blind source separation algorithm, a virtual multichannel was constructed by addition of each channel signal with a certain time delay. The mathematical expression for this is as follows [23]:

$$x_j(t) = x(t + (j-1)\tau), \tag{11}$$

where x_j is the virtual channel signal at time delay τ. The response of each virtual sensor is constructed as h_j, and then the virtual receiving matrix can be expressed as

$$y(t) = \begin{bmatrix} x(t) * h_1 \\ x(t+\tau) * h_2 \\ \vdots \\ x(t+(m-1)\tau) * h_m \end{bmatrix}. \tag{12}$$

In practical application, the parametric array data were extended to three channels. Then, the source signal was estimated using the FastICA algorithm. Based on the approach of estimating the SNR based on the frequency spectrum and comparing the frequency spectrum energy, the signal with larger SNR was extracted as the desired signal. For details of this simulation, the reader is referred to Guo et al. [24]. The results show that the SNR processed by this method is slightly worse than that obtained with correlation filter processing. However, correlation filter processing widens the time width of the received pulse signal, blurring details in the diagram, whereas the method used here preserves the detailed features of the original signal. Similar results were obtained when processing offshore experimental data, as described in the following section.

4. Sea Trials

To verify the effectiveness and characteristics of broadband parametric array technology for sub-bottom profiling in shallow seas, experiments were carried out in the Zhoushan area of the East China Sea from July 18 to 20, 2014. The parametric array system used was assembled using the same parametric array equipment as for the tank experiments, as shown in Figure 7.

In the sea trials, the broadband difference frequency signal used was the linear frequency modulation signal. The frequency modulation range for the emission signal envelope was 4–12 kHz. For the LFM difference frequency signal obtained by demodulation, the frequency range should be 8–24 kHz. The signal was emitted three times per second, and the sampling frequency was 224.7 kHz. The noise source was mainly line spectrum noise generated by the engines of the trial vessel. The received difference frequency echo signal first passed through the filter and was then processed by the single-channel blind signal separation algorithm. Finally, the signal from the seabed was obtained. Figure 7 shows the profile of a sandy seabed in a shallow sea using a pulse signal with a frequency modulation duration of 0.75 ms.

Figure 8 shows a clear layered structure. The original signal includes obvious line spectrum noise. Through processing by the single-channel blind signal separation algorithm, the noise was dramatically suppressed, while the details of the source signal were maintained. Detection of the sandy bottom by the equipment was good.

With regard to sub-bottom profiling, experiments were also carried out to detect buried objects on the seabed. In this region, pipelines have been laid on the seabed; some of the pipelines were covered with cement when laid, but others were not. Generally, the burial depth was less than 3 m. When detecting a subsea pipeline, the emission signal

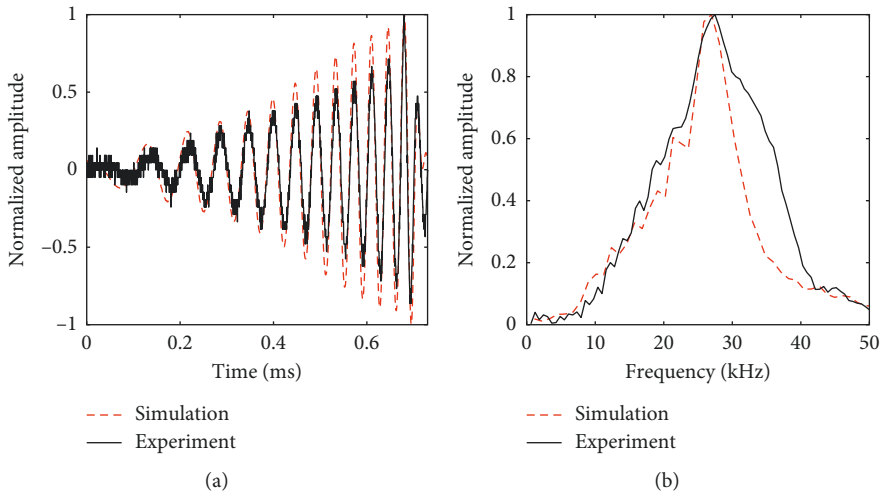

Figure 6: Time-domain waveform and spectra of the difference frequency signal. The simulation results were calculated based on the KZK equation.

Figure 7: Parametric array equipment used for sea trials.

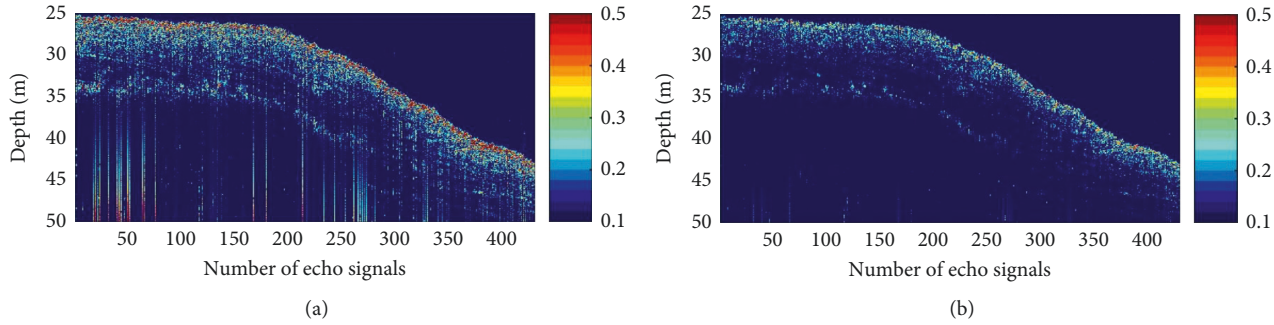

Figure 8: Seabed profile. (a) The original signal. (b) The result of single-channel blind signal separation processing.

envelope frequency was 9 kHz, and the duration was 0.8 ms. The signal was emitted three times per second, and the demodulation signal frequency of the difference frequency should be 18 kHz. The received echo difference frequency signal first passes through the filter and then is correlation processed. Finally, the envelope is obtained by Hilbert transform, and pseudocolor images are obtained. Figure 9 shows the pipeline detection results.

According to the detection results, it can be concluded that the pipeline is fully buried and that the burial depth is about 0.8 m. There is no cement around the measurement position. Investigation revealed that the pipeline was utility piping newly laid on the seabed in recent years. The parametric array survey can reveal whether a pipeline is buried, as well as its buried state. Furthermore, the burial depth can be estimated.

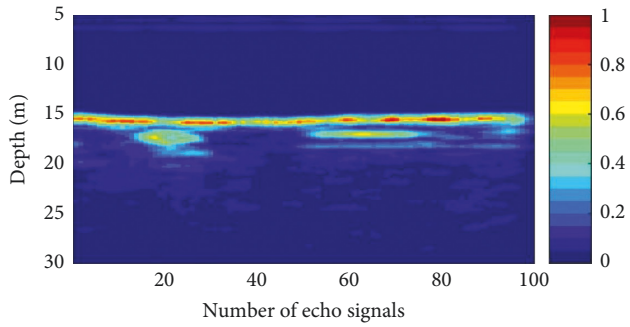

Figure 9: Pipeline detection.

5. Conclusions

This paper has discussed the use of a broadband parametric array for sub-bottom profiling. The fundamentals of broadband parametric array technology were introduced, and a set of broadband parametric array systems was designed. Through tank experiments, a performance evaluation was carried out on the system's directivity, source level, and parametric array length. The system possessed the following characteristics: (1) with a small transducer aperture, a broadband beam with low frequency, high directivity, and without sidelobes was realized; (2) parametric array lengths of less than 20 m were found to be well adapted to offshore detection; (3) compared with the double-frequency parametric array, there were certain advantages in the difference frequency signal gain and in high-resolution detection; (4) by combining the proposed method with a single-channel blind signal separation algorithm, the SNR of the echo signal could be substantially improved. In sea trials, the results of sub-bottom profiling and buried pipeline detection verified the effectiveness of the system for seafloor detection in shallow seas.

Data Availability

The data used to support the findings of this study are available from the corresponding author upon request.

Conflicts of Interest

The authors declare that there are no conflicts of interest regarding the publication of this paper.

Acknowledgments

This study was supported by the Excellent Young Teachers Program of GDOU (HDYQ2015010) and the Natural Science Foundation of Guangdong Province (2014A030310256).

References

[1] D. T. Blackstock, "Early years of the parametric array-An anecdotal history," *The Journal of the Acoustical Society of America*, vol. 125, no. 4, p. 2687, 2009.

[2] P. J. Westervelt, C. H. Allen, and R. S. Lansil, "Parametric end-fire array," *The Journal of the Acoustical Society of America*, vol. 32, no. 7, p. 934, 1960.

[3] P. J. Westervelt, "Parametric acoustic array," *The Journal of the Acoustical Society of America*, vol. 35, no. 4, pp. 535–537, 1963.

[4] H. O. Berktay, "Possible exploitation of non-linear acoustics in underwater transmitting applications," *Journal of Sound and Vibration*, vol. 2, no. 4, pp. 435–461, 1965.

[5] J. Chen, B. Zou, R. Wang, and S. A. Laboratory, "Research on wideband parametric acoustic sonar for submarine detection," *Journal of Huazhong University of Science and Technology*, vol. 42, no. 10, pp. 15–18, 2014.

[6] G. Shui, "Non-destructive evaluation of fatigue damage of train spring using nonlinear ultrasonic method," *Acta Acustica*, vol. 38, no. 5, pp. 570–575, 2013.

[7] C. P. Keravnou and M. A. Averkiou, "Parametric array for tissue harmonic imaging," *The Journal of the Acoustical Society of America*, vol. 140, no. 4, p. 3368, 2016.

[8] O. R. Godo, K. G. Foote, J. Dybedal, E. Tenningen, and R. Patel, "Detecting atlantic herring by parametric sonar," *Journal of the Acoustical Society of America*, vol. 127, no. 4, pp. EL153–EL159, 2010.

[9] K. G. Foote, R. Patel, and E. Tenningen, "Target-tracking in a parametric sonar beam, with applications to calibration," in *Proceedings of Oceans 2010 Mts/IEEE Seattle*, pp. 1–7, Seattle, WA, USA, September 2010.

[10] Y. Hwang, Y. Je, J. Lee et al., "Development of a multi-resonance transducer for highly directional underwater communication," *The Journal of the Acoustical Society of America*, vol. 134, no. 5, p. 4186, 2013.

[11] J. Zhang, X. Guangping, and T. Shengyu, "Parametric array differential pattern time delay shift coding underwater acoustic communication in the under-ice environment," *Acta Acustica*, vol. 35, no. 4, pp. 431–439, 2016.

[12] N. P. Chotiros, A. M. Mautner, A. Lovik, A. Kristensen, and O. Bergem, "Acoustic penetration of a silty sand sediment in the 1-10-KHz band," *IEEE Journal of Oceanic Engineering*, vol. 22, no. 4, pp. 604–615, 1997.

[13] V. F. Humphrey, S. P. Robinson, J. D. Smith et al., "Acoustic characterization of panel materials under simulated ocean conditions using a parametric array source," *The Journal of the Acoustical Society of America*, vol. 124, no. 2, pp. 803–814, 2008.

[14] L. A. Ostrovsky, "Research on parametric arrays in Russia: historical perspective," *Journal of the Acoustical Society of America*, vol. 125, no. 4, p. 2688, 2009.

[15] L. D. Marcoberardino, J. Marchal, and P. Cervenka, "Non-linear multi-frequency generation for underwater application," *Applied Acoustics*, vol. 73, no. 9, pp. 900–903, 2012.

[16] E. V. Dontsov and B. B. Guzina, "On the KZK-type equation for modulated ultrasound fields," *Wave Motion*, vol. 50, no. 4, pp. 763–775, 2013.

[17] M. Cervenka and M. Bednarik, "Non-paraxial model for a parametric acoustic array," *The Journal of the Acoustical Society of America*, vol. 134, no. 2, p. 933, 2013.

[18] Y. Je, H. Lee, K. Been, and W. Moon, "A micromachined efficient parametric array loudspeaker with a wide radiation frequency band," *The Journal of the Acoustical Society of America*, vol. 137, no. 4, pp. 1732–1743, 2015.

[19] H. Ahn, Y. Hwang, and W. Moon, "Underwater parametric array source transducer composed of pzt rods and thin polymer plate with high power efficiency for wideband sound generation," *The Journal of the Acoustical Society of America*, vol. 140, p. 3089, 2016.

[20] Y. Hwang, H. Ahn, D.-N. Nguyen, W. Kim, and W. Moon, "An underwater parametric array source transducer composed of pzt/thin-polymer composite," *Sensors and Actuators A: Physical*, vol. 279, pp. 601–616, 2018.

[21] H. M. Merklinger, "Improved efficiency in the parametric transmitting array," *The Journal of the Acoustical Society of America*, vol. 58, no. 4, pp. 784–787, 1975.
[22] M. B. Moffett and R. H. Mellen, "Effective lengths of parametric acoustic sources," *The Journal of the Acoustical Society of America*, vol. 70, no. 5, pp. 1424–1426, 1981.
[23] A. Hyvärinen and E. Oja, "Independent component analysis: algorithms and applications," *Neural Networks*, vol. 13, no. 4-5, pp. 411–430, 2000.
[24] Y. Guo, B. Zou, J. Chen, R. Wang, and S. A. Laboratory, "Application of single channel blind signal separation algorithm on profile data processing," *Journal of Test and Measurement Technology*, vol. 30, no. 1, pp. 51–56, 2016.